

# Electronic Supplementary Information

## A High Voltage Layered Cathode Framework for Rechargeable Potassium-Ion Battery : P2-Type $\text{K}_{2/3}\text{Ni}_{1/3}\text{Co}_{1/3}\text{Te}_{1/3}\text{O}_2$

Titus Masese<sup>a\*</sup>, Kazuki Yoshii<sup>a</sup>, Minami Kato<sup>a</sup>, Keigo Kubota<sup>b</sup>, Zhen-Dong Huang<sup>c</sup>, Hiroshi Senoh<sup>a</sup> and Masahiro Shikano<sup>a</sup>

<sup>a</sup> Research Institute of Electrochemical Energy, Department of Energy and Environment (RIECEN), National Institute of Advanced Industrial Science and Technology (AIST), 1-8-31 Midorigaoka, Ikeda, Osaka 563-8577, JAPAN

<sup>b</sup> AIST-Kyoto University Chemical Energy Materials Open Innovation Laboratory (ChEM-OIL), Sakyo-ku, Kyoto 606-8501, JAPAN

<sup>c</sup> Key Laboratory for Organic Electronics and Information Displays and Institute of Advanced Materials (IAM), Nanjing University of Posts and Telecommunications (NUPT), Nanjing, 210023, CHINA

\*Correspondence to: Titus Masese (Lead contact) ([titus.masese@aist.go.jp](mailto:titus.masese@aist.go.jp)) and Zhen-Dong Huang ([iamzdhuang@njupt.edu.cn](mailto:iamzdhuang@njupt.edu.cn))

## Experimental

### 1.1 Synthesis

Polycrystalline samples of  $\text{K}_2\text{NiCoTeO}_6$  were synthesised via the conventional solid-state reaction. A stoichiometric mixture of CoO (High Purity Chemicals, purity of 99%),  $\text{TeO}_2$  (Aldrich, purity of  $\geq 99.0\%$ ),  $\text{K}_2\text{CO}_3$  (Rare Metallic, 99.9%) and NiO (High Purity Chemicals, purity of 99%) was thoroughly pulverised, then pelletised and subsequently calcined at 800 °C in a muffle furnace for 24 hours in air. Thereafter, the furnace was cooled to ambient temperature at a rate of 10 °C/h.  $\text{K}_2\text{NiCoTeO}_6$  was formed as a microcrystalline orange-brown powder. To protect the material against moisture exposure, the as-prepared  $\text{K}_2\text{NiCoTeO}_6$  samples were transferred into a glove box (Ar-purged) as soon after removing from the furnace.

### 1.2 X-ray diffraction (XRD) analyses

Synchrotron X-ray diffraction (SXRD) measurements were performed at SPring-8 (Hyogo, Japan) using BL19B2 beam line at 298 K (with a wavelength of 0.500212(2) Å in the  $2\theta$  range from 0° to 50° at a step size of 0.01° with Debye–Scherrer geometry). Analysis of data was done using the Rietveld refinement protocol implemented in the JANA 2006 program and the crystal structure visualisation was done using VESTA software. Structural refinements of  $\text{K}_2\text{NiCoTeO}_6$  were performed on crystal data based on the  $\text{Na}_2\text{Ni}_2\text{TeO}_6$  (adopting the centrosymmetric  $P6_3/mcm$  space group) structural model. The structure was refined using 17 terms of Legendre polynomials to describe the background and with a damping factor set at 0.1. The pseudo-Voigt profile function and Berar-Baldinozzi method for asymmetry correction were applied. Preferred orientation along the (00 $l$ ) axis was also taken into account. Further details pertaining to the refined structures can

be retrieved from the Fachinformationszentrum Karlsruhe, D-76344 Eggenstein-Leopoldshafen (Germany), under the accession number CSD-434033.

Complementary information about the phase evolution during cycling was obtained from conventional *ex situ* XRD studies performed on  $\text{K}_{2/3}\text{Ni}_{1/3}\text{Co}_{1/3}\text{Te}_{1/3}\text{O}_2$  using a series of equivalent K-half cells that were cycled to different states of (dis)charge. Cells were then disassembled / dismantled in an argon-filled glovebox with the cathode material being scraped off and washed thoroughly using super dehydrated acetonitrile to completely remove any remanent electrolyte (*i.e.*, ionic liquid).

### **1.3 Morphological and elemental characterisations**

Morphologies of the product powder were analysed by both scanning and transmission electron microscope (JSM-6510LA and TITAN80-300F, respectively). Samples for high resolution TEM (hereafter as HRTEM) were dispersed in alcohol by ultrasonification and loaded on to a holey grids for imaging on a TITAN80-300F at an accelerated voltage of 200 kV without exposure to neither air nor moisture. HRTEM image simulations were performed with the JEMS 31(PECD) software. Chemical quantifications were determined by inductively-coupled plasma absorption electron spectroscopy (ICP-AES) on a Shimadzu ICPS-8100 instrument.

### **1.4 Thermal analyses**

Thermogravimetric analysis and related analyses were performed using a TG-DTA instrument 2020SA (Bruker AXS) in the temperature range of 30–900°C under Ar (with a ramp rate of 5 °C min<sup>-1</sup>). A baseline correction of the TG curve was done, prior to each measurement, by measuring the empty crucible.

### **1.5 Theoretical calculations**

To visualise the  $K^+$  conduction trajectories in the  $K_2NiCoTeO_6$  structure, bond valency energy landscape (BVEL) calculations were performed using the bond valency parameters developed by Adams and co-workers.<sup>1</sup> The parameters take into consideration the polarisability of the mobile cations, in this case  $K^+$ , and the influence of the counter ions of the structure up to a distance of 10 Å.

## 1.6 Electrochemical measurements

CR2032-type coin cells were used to assess the electrochemical performance of  $K_2NiCoTeO_6$ . K metal was used as the counter electrode. Assembly of the coin cells was performed inside an argon-purged glove box (water and oxygen content was maintained at < 0.1 ppm). For fabrication of the composite electrode, the  $K_2NiCoTeO_6$  composite was mixed with polyvinylidene fluoride (binder) and carbon black to attain a final weight ratio of 85:7.5:7.5 (active material:85%). A viscous slurry was made using N-methyl-2-pyrrolidinone (purity of 99.5%, Sigma Aldrich), which was then cast on aluminium foil. The loading used was typically in the range of 4–5 mg cm<sup>-2</sup>. Composite electrodes were punched and dried *in vacuo* at 120 °C. A 0.5 M potassium bis(trifluoromethanesulfonyl)imide (hereafter as KTFSI) in N-methyl-N-propylpyrrolidinium bis(trifluoromethane sulfonyl)imide (Pyr<sub>13</sub> TFSI) (Kanto Chemicals (Japan), 99.9%, <20 ppm H<sub>2</sub>O) ionic liquid was used as the electrolyte. Glass fiber separators were used to separate the electrodes, which had been dried *in vacuo* at 300 °C for 24 h. Cyclic voltammetry tests were conducted within a voltage window of 2.8–4.7 V, whilst galvanostatic (dis)charge tests (or technically, cycling) were done at a voltage range of 1.3–4.7 V (*versus*  $K^+/K$ ). Unless otherwise stated, all the measurements were conducted at room temperature (25 °C).

## **1.7 X-ray absorption spectroscopy (XAS)**

To ascertain the valency state of the constituent transition metal elements in  $\text{K}_2\text{NiCoTeO}_6$ , Co *K*-edge and Ni *K*-edge X-ray absorption spectroscopy (XAS) measurements were conducted on pelletised samples. CoO and NiO (reference compounds) were also prepared as homogeneous pellets. The XAS spectra were measured in the Ni and Co *K*-edges energy region at room temperature in transmission mode at a laboratory XAS facility.

**Table S1.** Atomic coordinates ( $x, y, z$ ), occupancies ( $g$ ), and isotropic atomic displacement parameters ( $U_{\text{iso}}$ ) obtained by Rietveld refinement of synchrotron X-ray diffraction data for as-prepared  $\text{K}_2\text{NiCoTeO}_6$  indexed in the space group  $P6_3/mcm$  (hexagonal) with lattice constants  $a = b = 5.1952(11) \text{ \AA}$ ,  $c = 12.5692(6) \text{ \AA}$ , and  $V = 293.79(1) \text{ \AA}^3$ . The agreement indices used are  $R_{\text{wp}} = [\sum w_i(y_{\text{io}} - y_{\text{ic}})^2 / \sum w_i(y_{\text{io}})^2]^{1/2}$ ,  $R_{\text{p}} = \sum |y_{\text{io}} - y_{\text{ic}}| / \sum y_{\text{io}}$  and the goodness of fit,  $\chi^2 = [R_{\text{wp}}/R_{\text{exp}}]^2$  where  $R_{\text{exp}} = [(N - P) / \sum w_i y_{\text{io}}^2]^{1/2}$ ,  $y_{\text{io}}$  and  $y_{\text{ic}}$  are the observed and calculated intensities,  $w_i$  is the weighting factor,  $N$  is the total number of  $y_{\text{io}}$  data when the background is refined, and  $P$  is the number of adjusted parameters. The occupancies of Ni and Co were fixed to values obtained from inductively-coupled plasma (ICP) measurements. The structure of  $\text{K}_2\text{NiCoTeO}_6$  was refined using the isotopic  $\text{Na}_2\text{Ni}_2\text{TeO}_6$  as the initial refinement model.<sup>2</sup>

Atom	$x$	$y$	$z$	$g$	$U_{\text{iso}}$
Te1	0	0	0	1	0.003(1)
Ni1	0.667	0.333	0	0.505	0.001(4)
O1	0.6731(4)	0.6731(4)	0.5924(8)	1	0.001(2)
K1	0.3501(6)	0	0.25	0.502(3)	0.017(1)
K2	0.333	0.667	0.25	0.198(2)	0.002(1)
Co1	0.667	0.333	0	0.485	0.001(4)

$$R_{\text{wp}}=5.65\% \quad R_{\text{p}}=4.61\% \quad \chi^2=1.89$$

\*  $g$  and  $U_{\text{iso}}$  denote the occupancy and isotropic thermal factor, respectively.

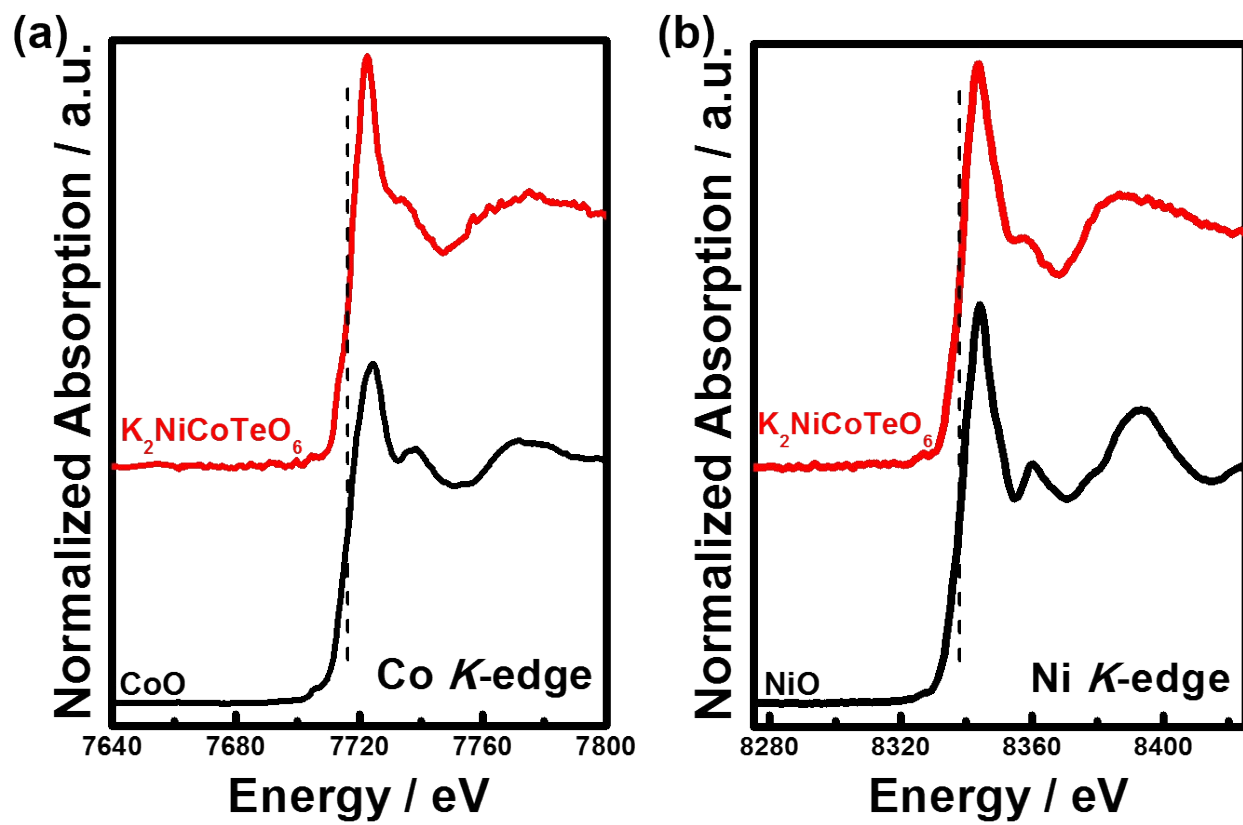


**Figure S1.** (a) Co *K*-edge and (b) Ni *K*-edge XANES spectra of  $K_2NiCoTeO_6$  along with selected compounds possessing  $Co^{2+}$  and  $Ni^{2+}$  in octahedral coordination (as references).

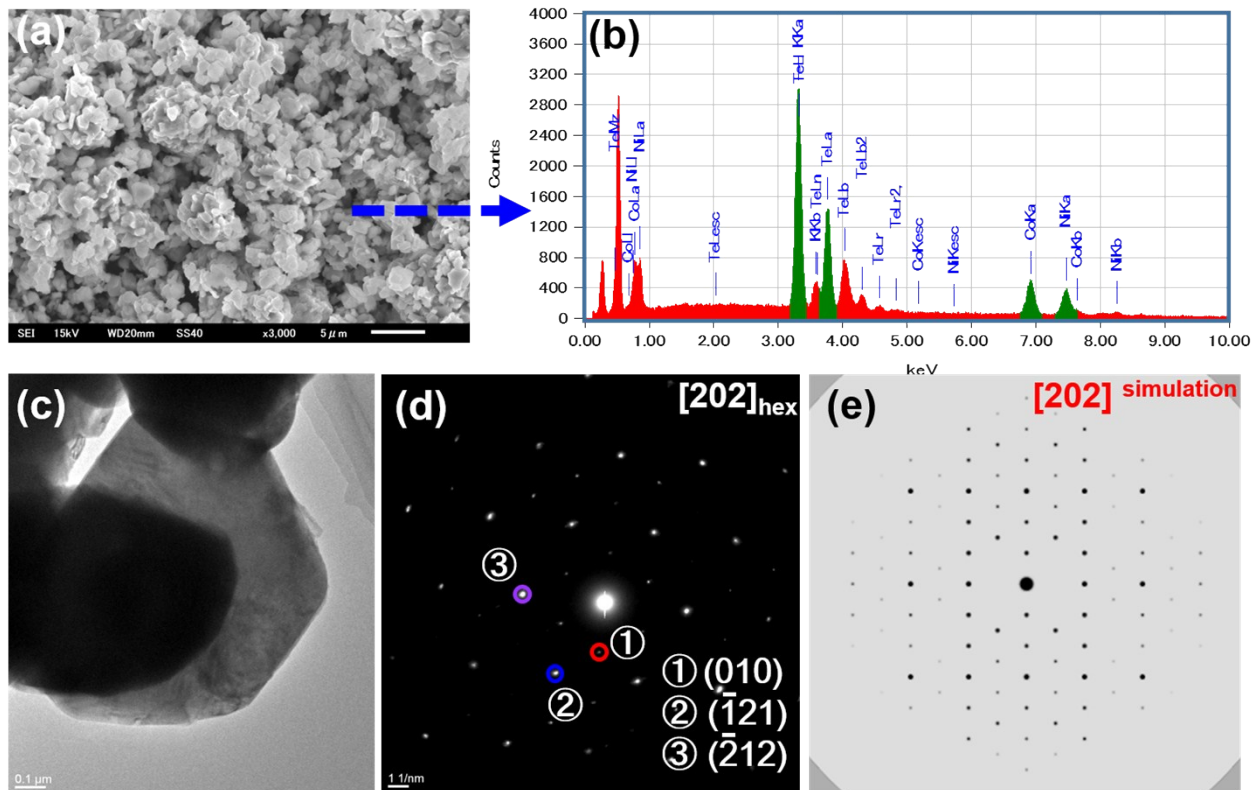


**Figure S2.** SEM picture of the  $K_2NiCoTeO_6$  powders (a) and the SEM-EDX spectrum of the powders (b). A bright-field TEM image of the majority particles (c) and the corresponding SAED pattern revealing an array of pseudo-hexagonal symmetry dots that could be indexed, using the hexagonal settings, as the  $[202]$  zone axis. Simulation of the electron diffraction pattern is provided in (e).

**Table S2.** Results of Inductively Coupled Plasma (ICP) measurements of  $\text{K}_2\text{NiCoTeO}_6$

<b>compound</b>	<b>K</b>	<b>Co / Ni</b>	<b>Te</b>
	<b>(mol wt%)</b>	<b>(mol wt%)</b>	<b>(mol wt%)</b>
$\text{K}_2\text{NiCoTeO}_6$	1.827	0.969/1.0096	1

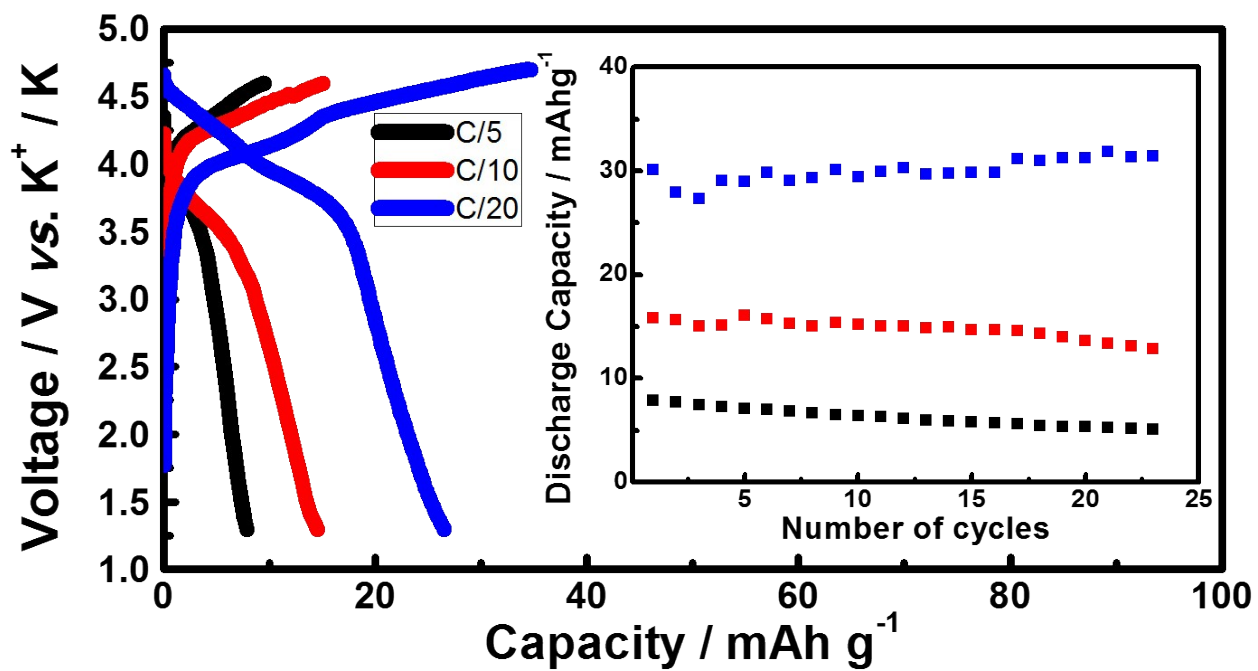


**Figure S3.** Voltage (dis)charge profiles of  $K_2NiCoTeO_6$  upon cycling at various current densities.

Inset shows the cycle performance at the corresponding current densities.

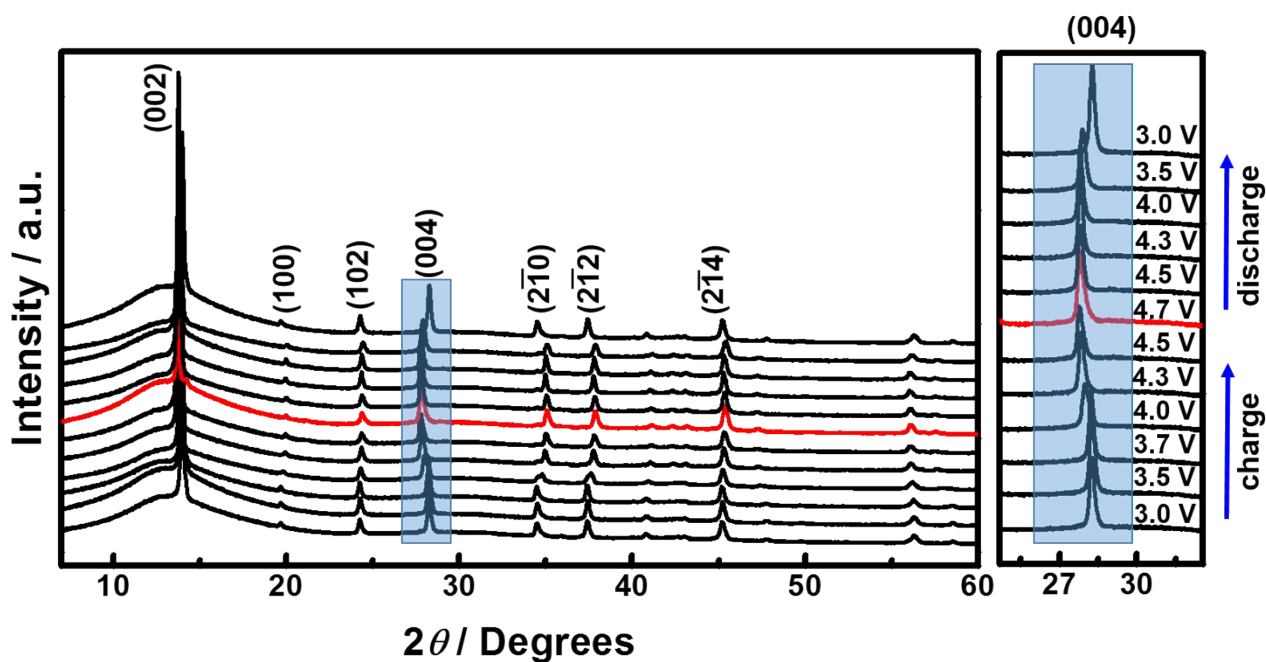


**Figure S4.** XRD *ex situ* patterns whilst  $\text{K}_2\text{NiCoTeO}_6$  is (dis)charged at a current density commensurate to  $C/20$  rate (20 h of (dis)charge), and the enlarged XRD pattern (shown in right) indicating peak shifts of the (004) Bragg diffraction peaks during (dis)charging. These results affirm topotactic potassium ion extraction and (re)insertion in  $\text{K}_2\text{NiCoTeO}_6$ .

A continuous shift of peak positions on cycling is evident, with the trend during K-ion extraction being reversed on reinsertion; indicating the full reversibility of K-ion (de)insertion process, as confirmed further by the remarkable similarity of the XRD patterns for the pristine and the discharged electrodes. The Bragg diffraction lines observed were univocally indexable to the hexagonal space group  $P6_3/mcm$ , suggesting no additional structural modification of the P2-type framework. In other words, P2-type framework is essentially retained. In particular, (00 $l$ ) Bragg peaks shift to lower  $2\theta$  diffraction angles upon charging, which arises by convention from increasing electrostatic repulsion between  $\text{NiO}_6/\text{CoO}_6$  and  $\text{TeO}_6$  layers which become less screened by K-ions upon K removal (extraction) and a *vice versa* trend prevails during discharging (K-ion reinsertion).

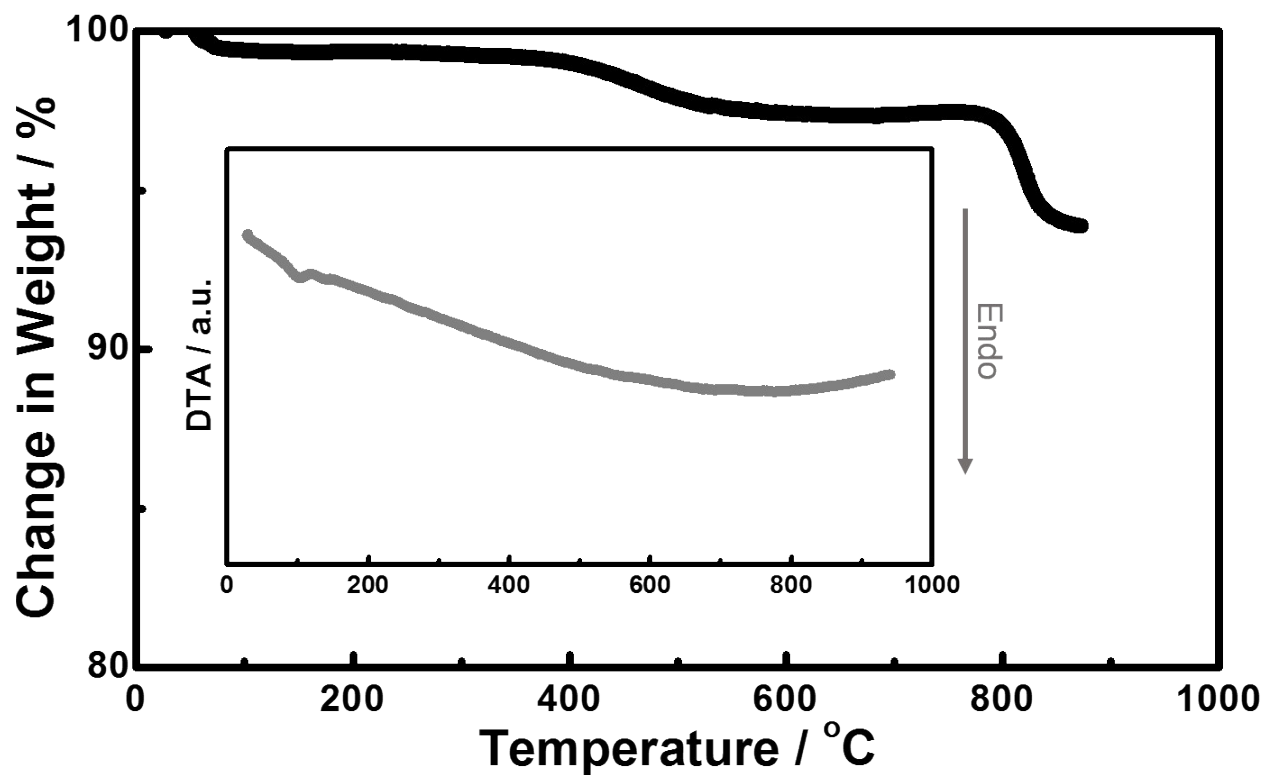


**Figure S5.** Thermogravimetry (TG) and differential thermal analysis (DTA) curves (inset) of  $\text{K}_2\text{NiCoTeO}_6$  ranging from 25°C to 950°C. The weight loss observed at around 100°C arises from water absorbed during the loading of the powders in Pt ampoules prior to measurements.

## (References)

1. S. Adams, *Solid State Ionics*, 2006, **177**, 1625.
2. M. A. Evstigneeva, V. B. Nalbandyan, A. A. Petrenko, B. S. Medvedev and A. A. Kataev, *Chem. Mater.*, 2017, **23(5)**, 1174.